Jefferson Lab Accelerator Seminar

Thursday, May 27, 2021
11:00 AM – 12:00 PM (EDT)

Loss Mechanisms on Superconducting Quantum Devices and Microwave Microscopy for Probing Superconducting Devices Metrology

Speaker: Tamin Tai

Acknowledgement:

Dr. Steven Anlage Group: Dr. Behnood Ghamsari, Jingnan Cai, Dr. Bakhron Oripov
Dr. Ben Palmer Group:Dr. S. Premaratne, Dr. Jen-Hao Yeh, Rui R. Zhang, Yizhou Huang
Dr. Frederick Wellstood Group: Dr. Sudeep Dutta, Cody Ballard

This work is primarily supported by DOE-BES (grant # DESC0018788)
and University of Maryland, Quantum Materials Center

Classical vs. Quantum computing

- Classical computing utilizes two voltage levels for computations (bits)

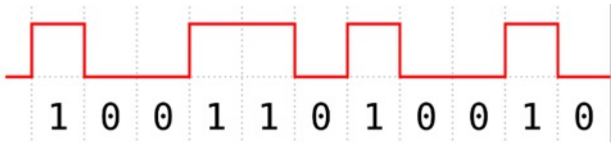

- Quantum superpositions can be used to speed up certain computations

$$\Psi = \alpha|0\rangle + \beta\,|1\rangle$$

(quantum bit)

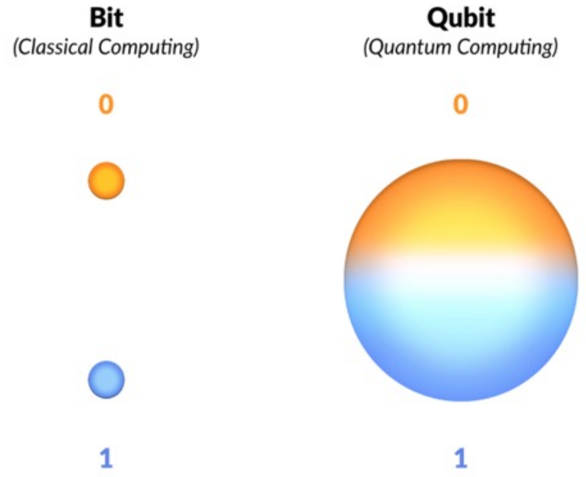

Superconducting quantum systems

IBM chip

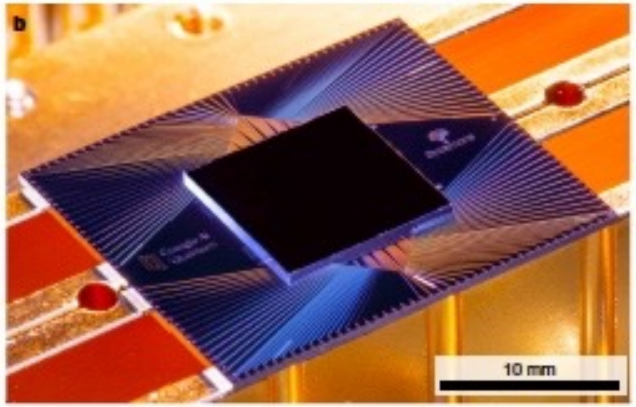

Google

Different Types of Superconducting Qubit

Remarkable improvement in T1 and T2

--- Materials

--- Design

--- Fabrication

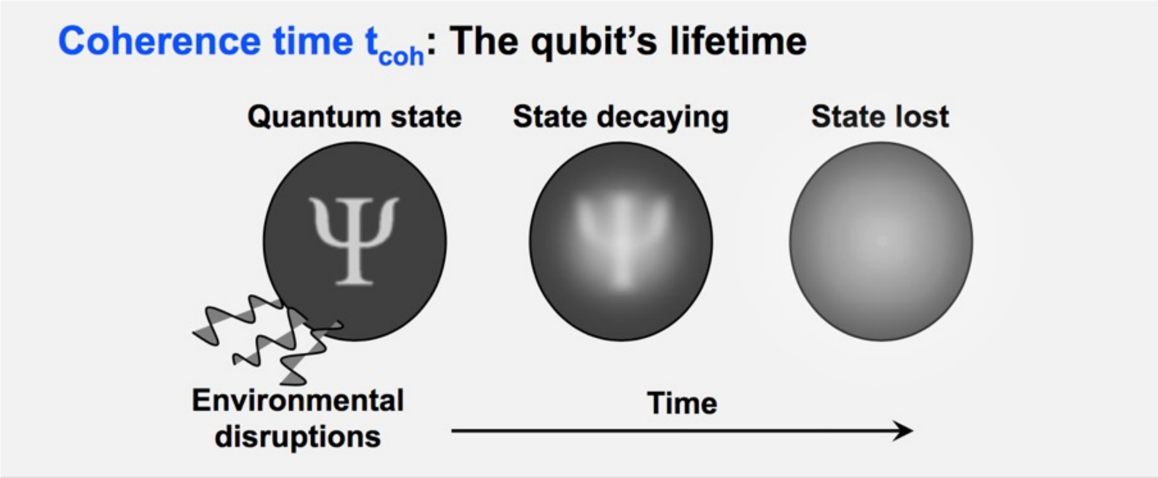

$$\frac{1}{T_2} = \frac{1}{2T_1} + \frac{1}{T_\phi}$$

Moore's law for T_2

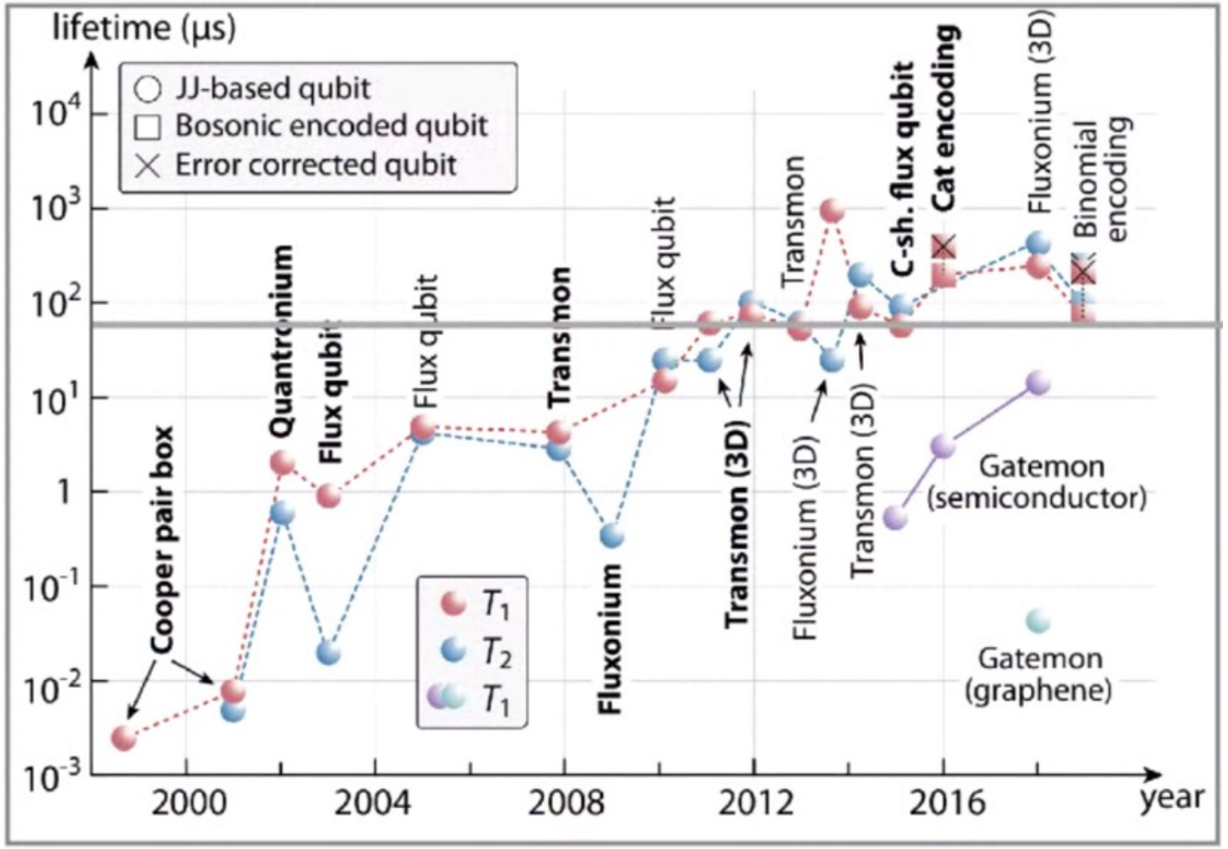

Kjaergaard *et al*, arXiv:1905.13641v1

M. Kjaergaard, WDO, et al., arXiv:1905.13641

P. Krantz, WDO, et al., Appl. Phys. Rev. 6, 021318 (2019); arXiv:1905.13641

WDO & Welander, MRS Bulletin (2013)

Harmonic Resonators

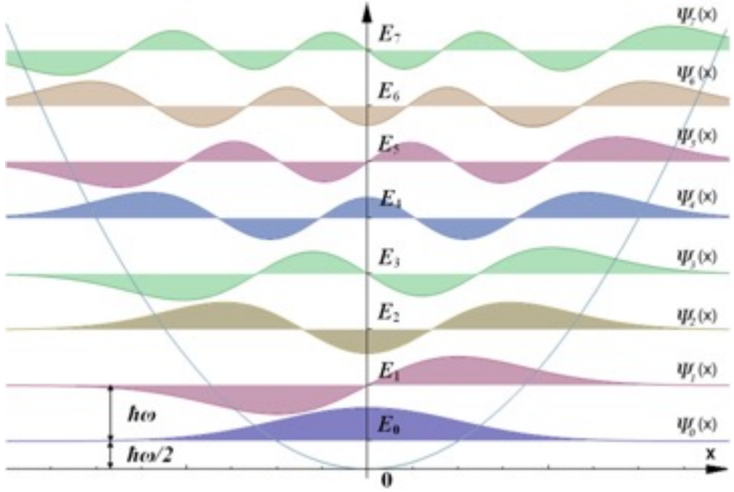

$$E_n = (n + \frac{1}{2})\hbar\omega$$

3D types of Cavities

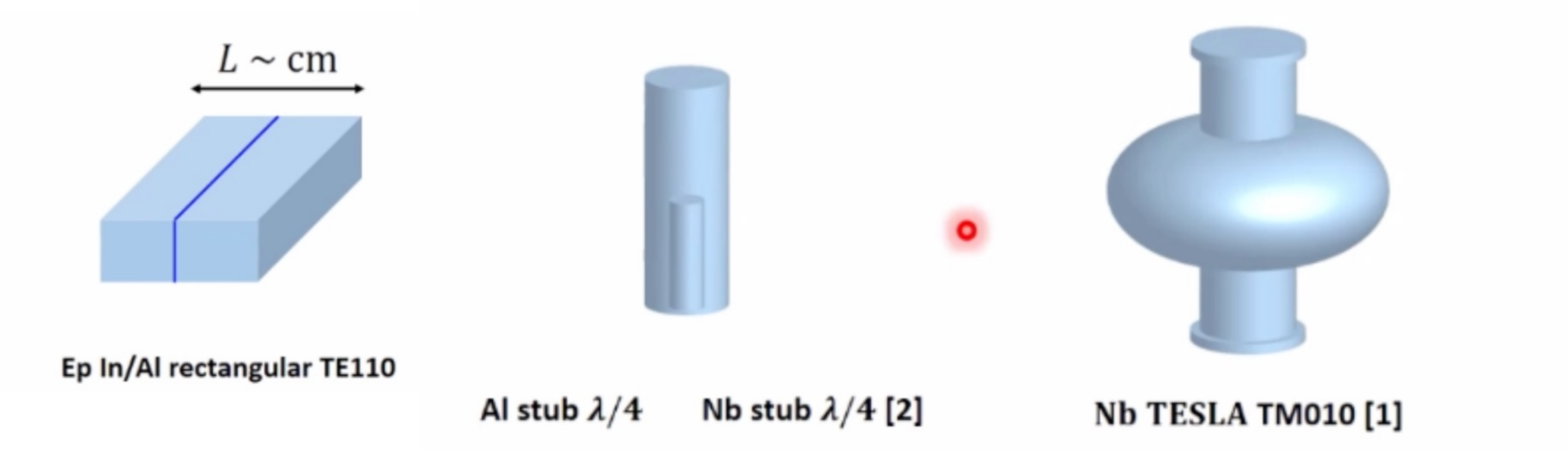

Planar types of Cavities

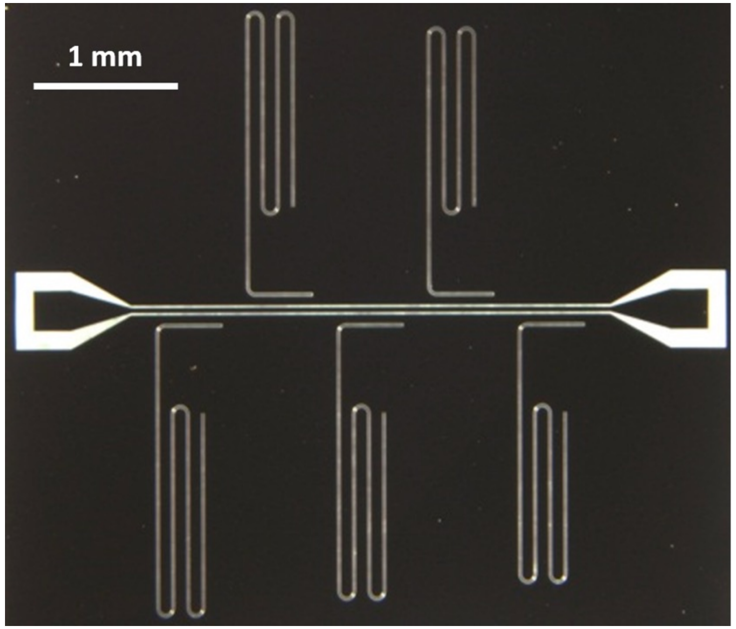

G. Calusine *et al. Appl. Phys. Lett.*, vol. 112, no. 6, pp. 1–7, 2018

λ/2 Resonator Design and Fabrication

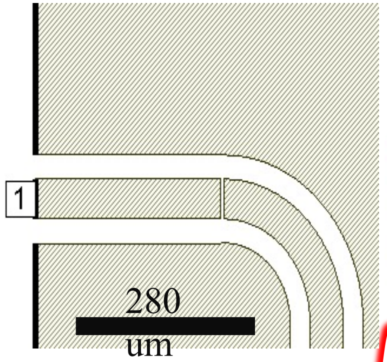

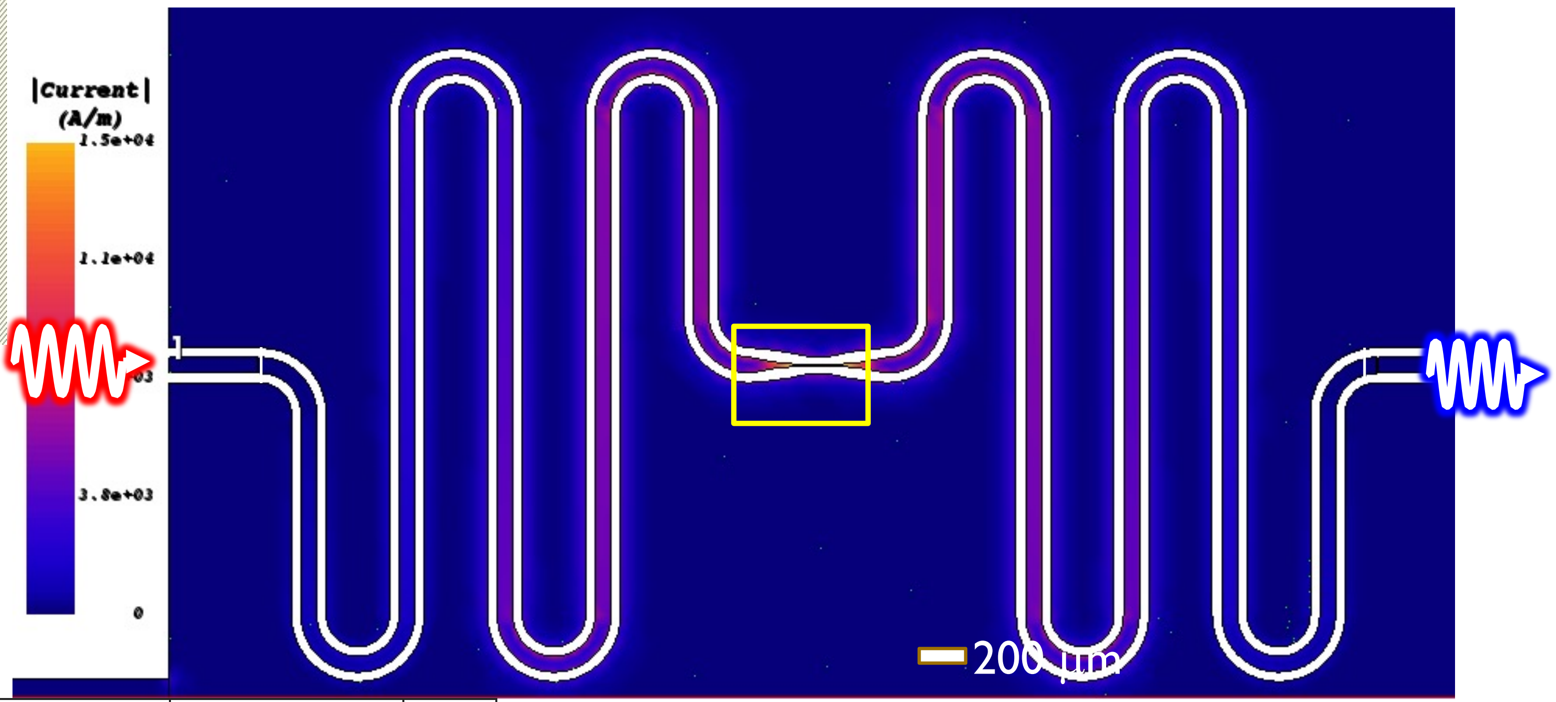

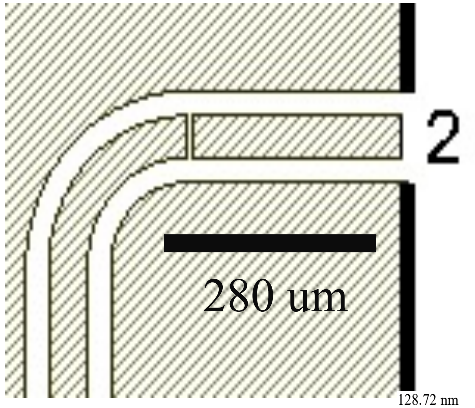

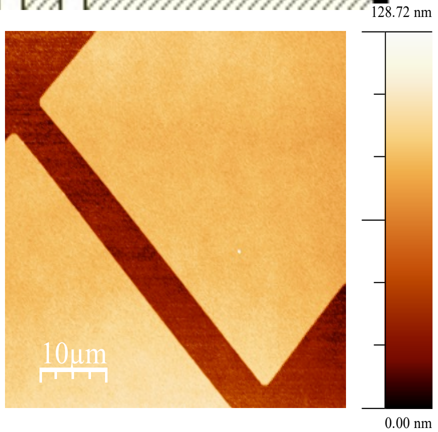

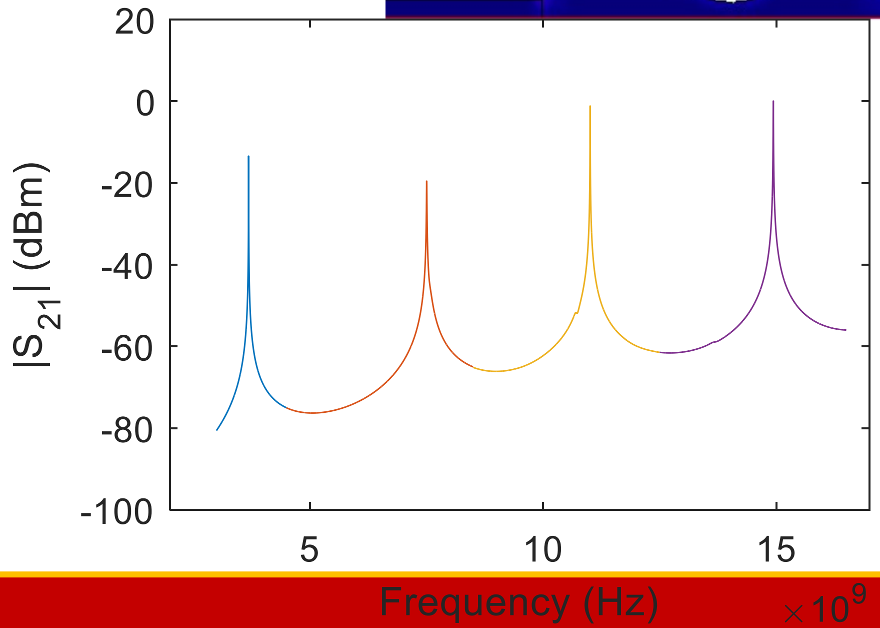

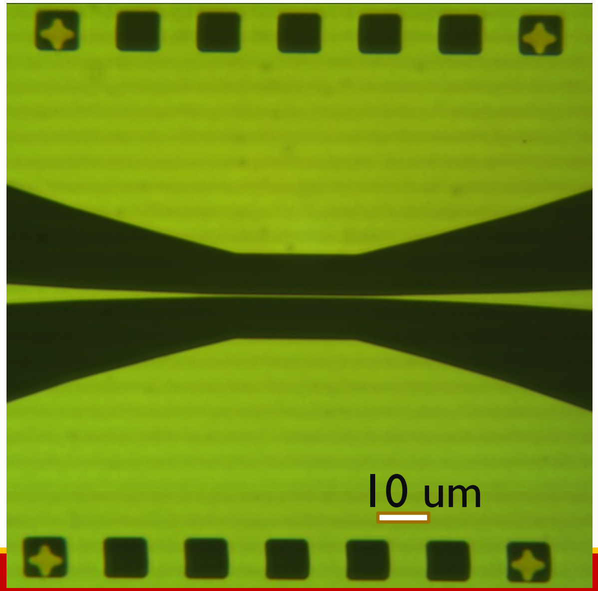

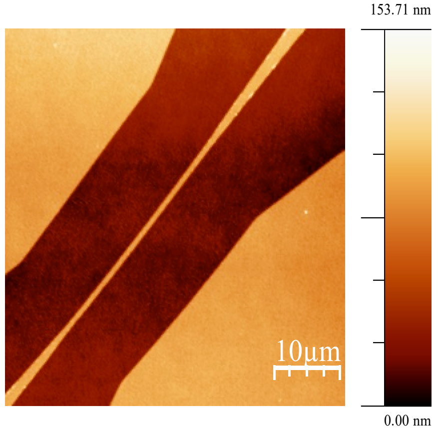

λ/2 Resonator Design and Fabrication

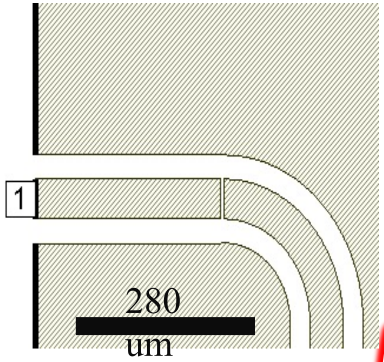

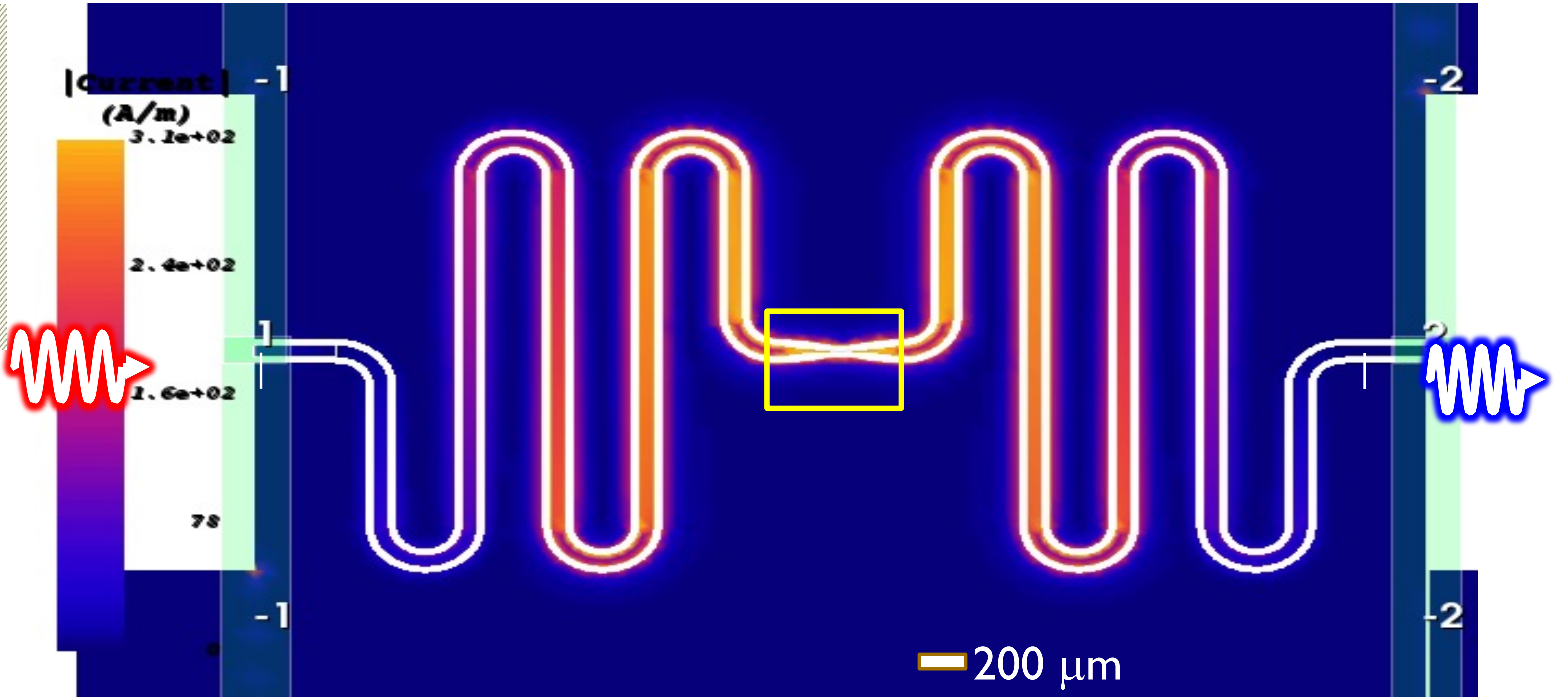

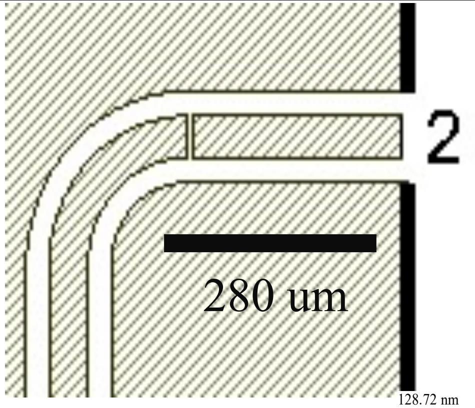

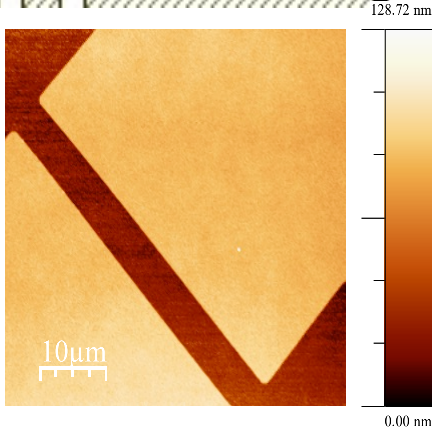

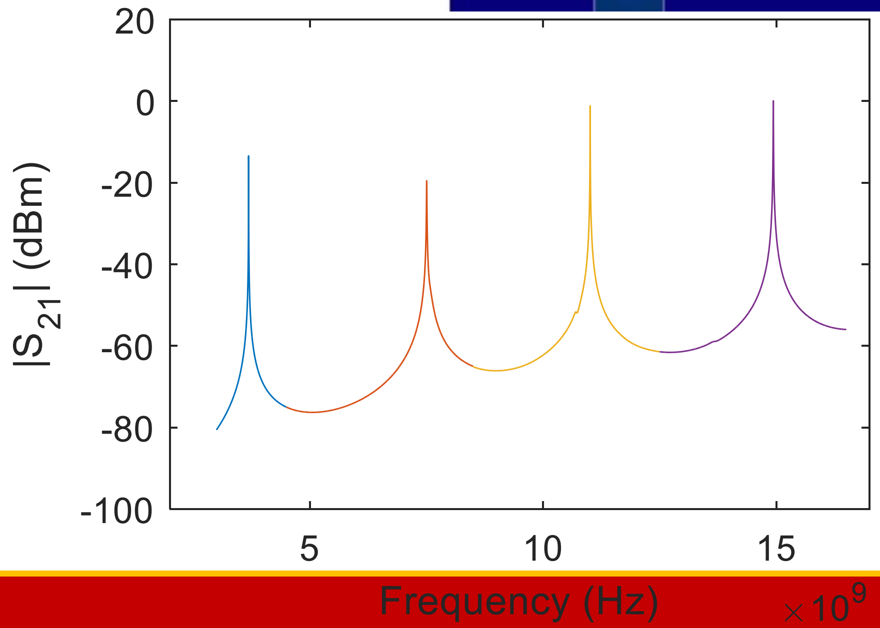

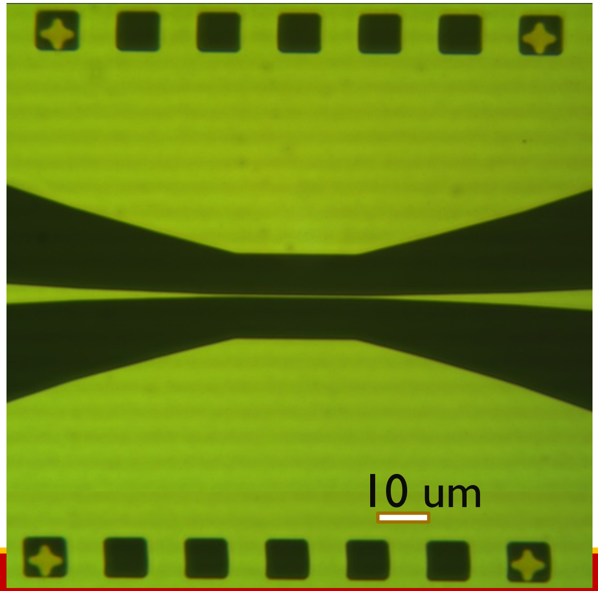

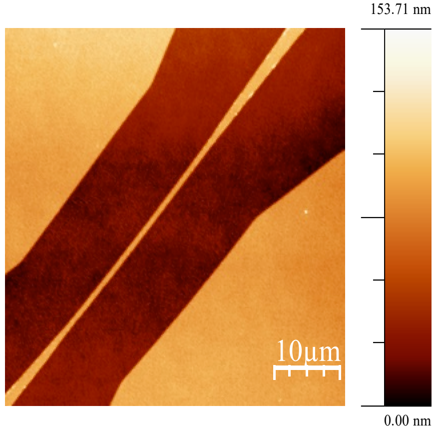

λ/2 Resonator Design and Fabrication

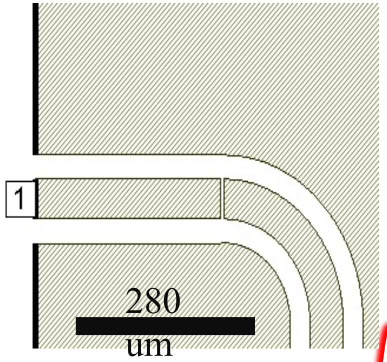

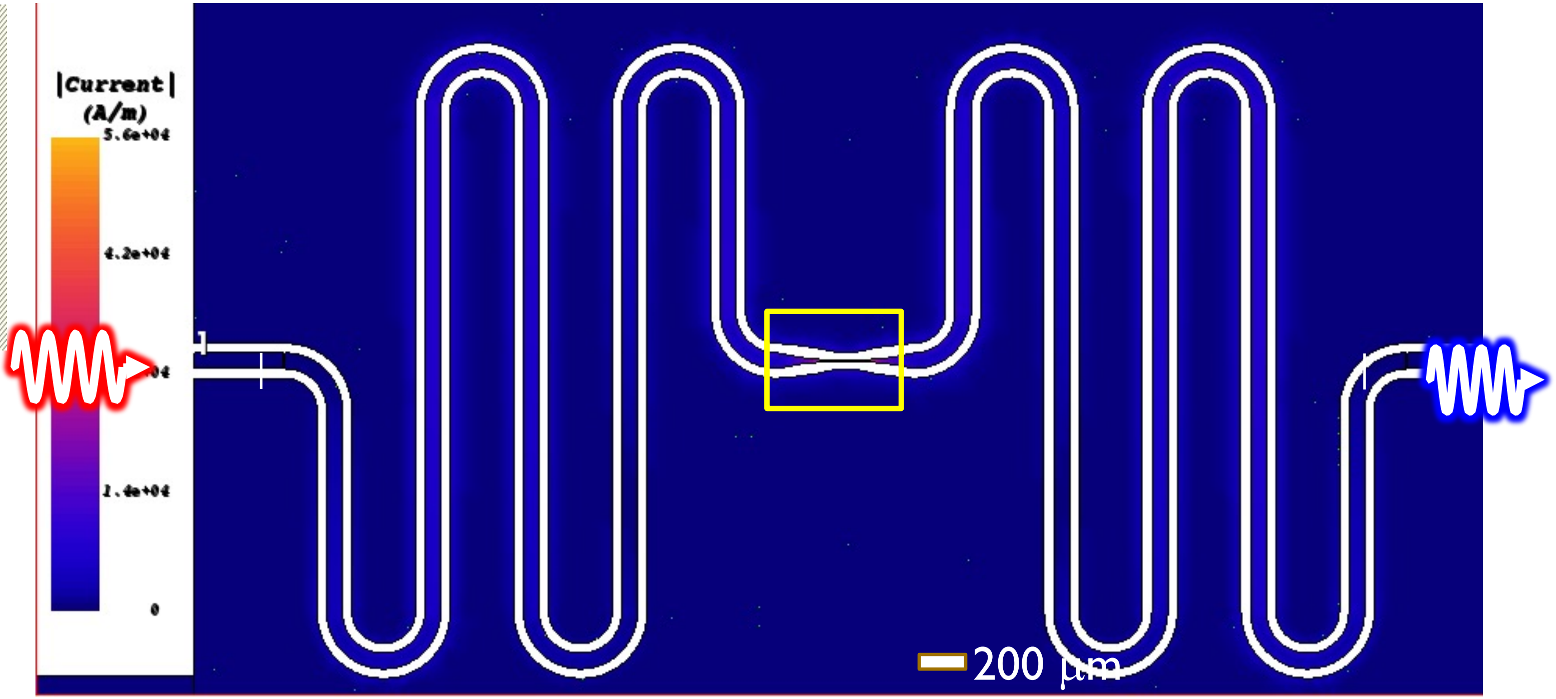

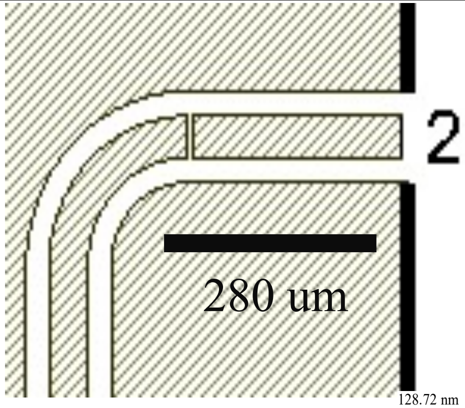

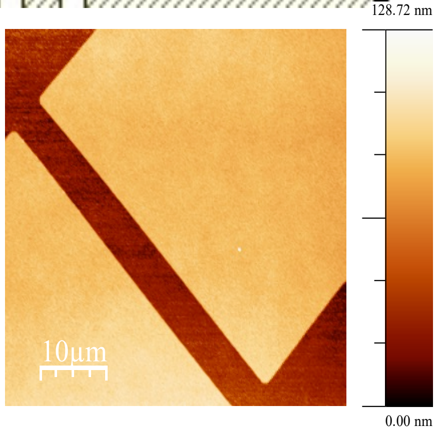

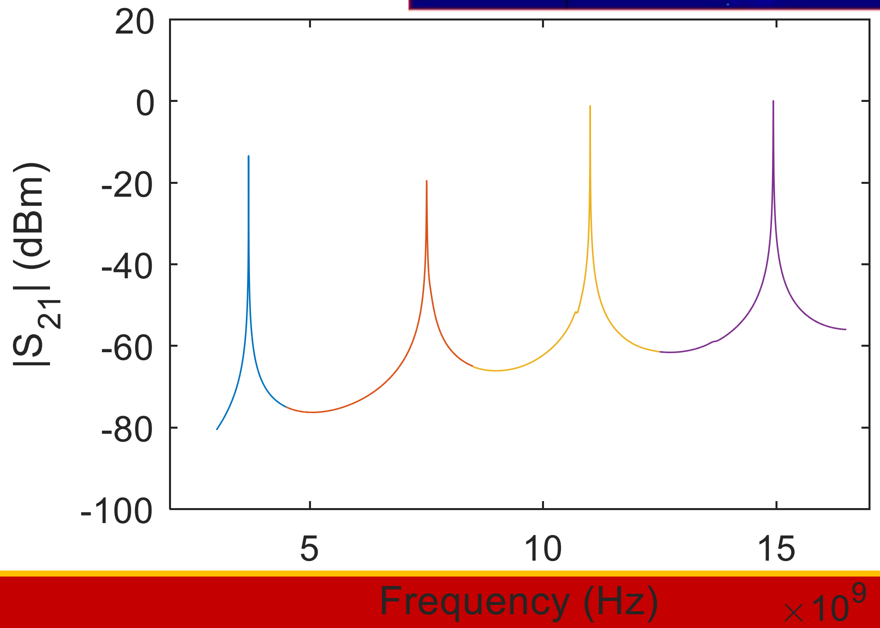

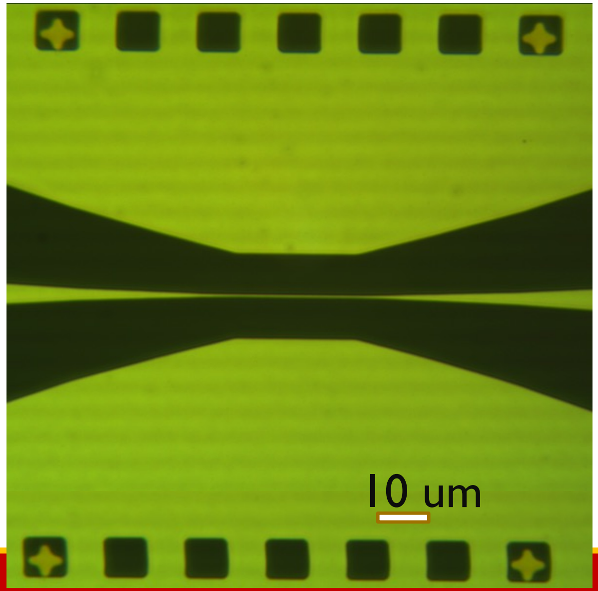

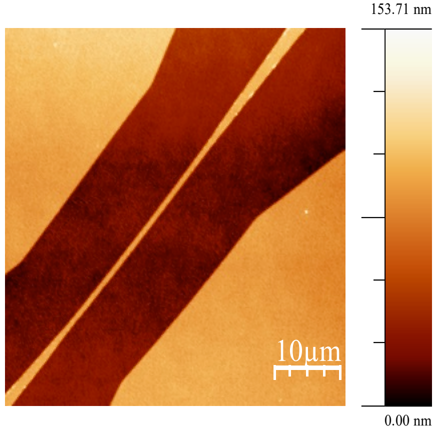

Packaging and System Setup

Indium GND

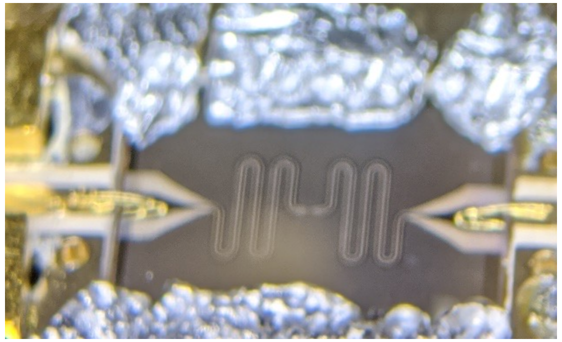

Packaging

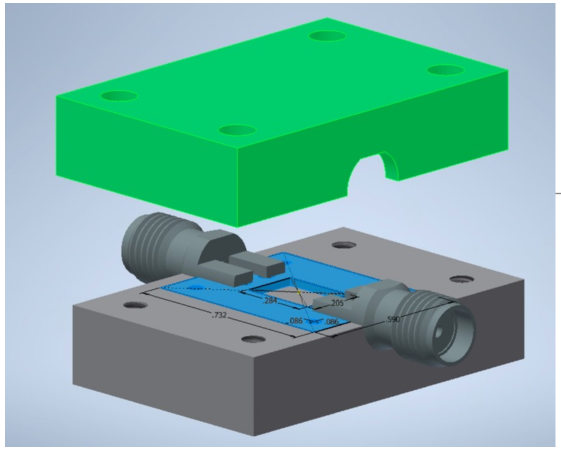

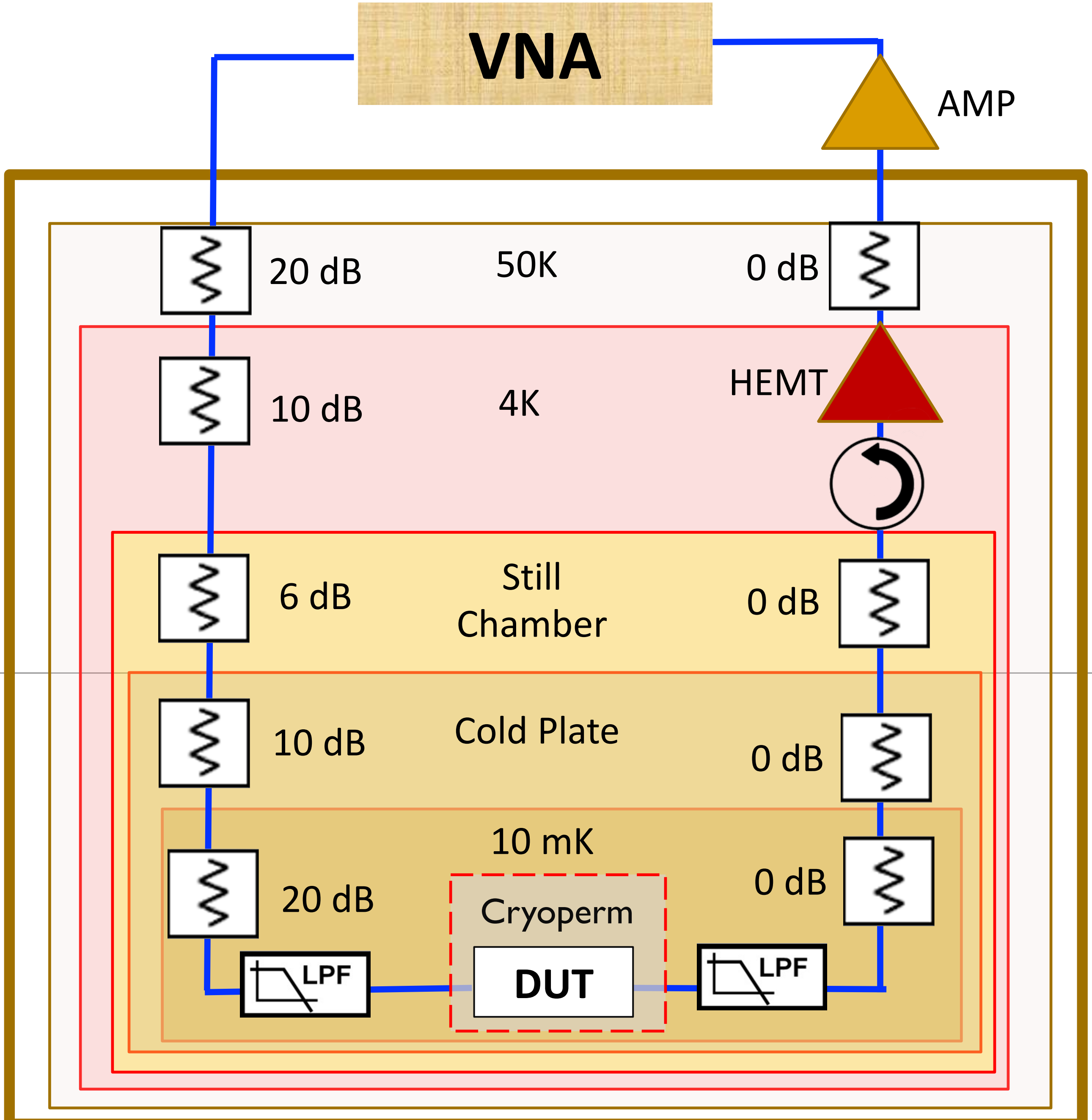

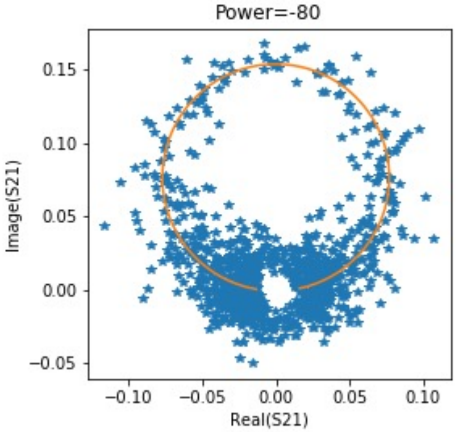

$$S_{21}(f) = |S_{21,in}||S_{21,out}| * \left(\frac{Q_L/Q_c}{1+2iQ_L\left(\frac{f-f_r}{f_r}\right)} + c_0\right)$$

=> Q_L and Q_c

$$\frac{1}{Q_L} = \frac{1}{\boldsymbol{Q_i}} + \frac{1}{Q_c}$$

Qc ~7e5
Q_L ~ Qi

Measurement Results

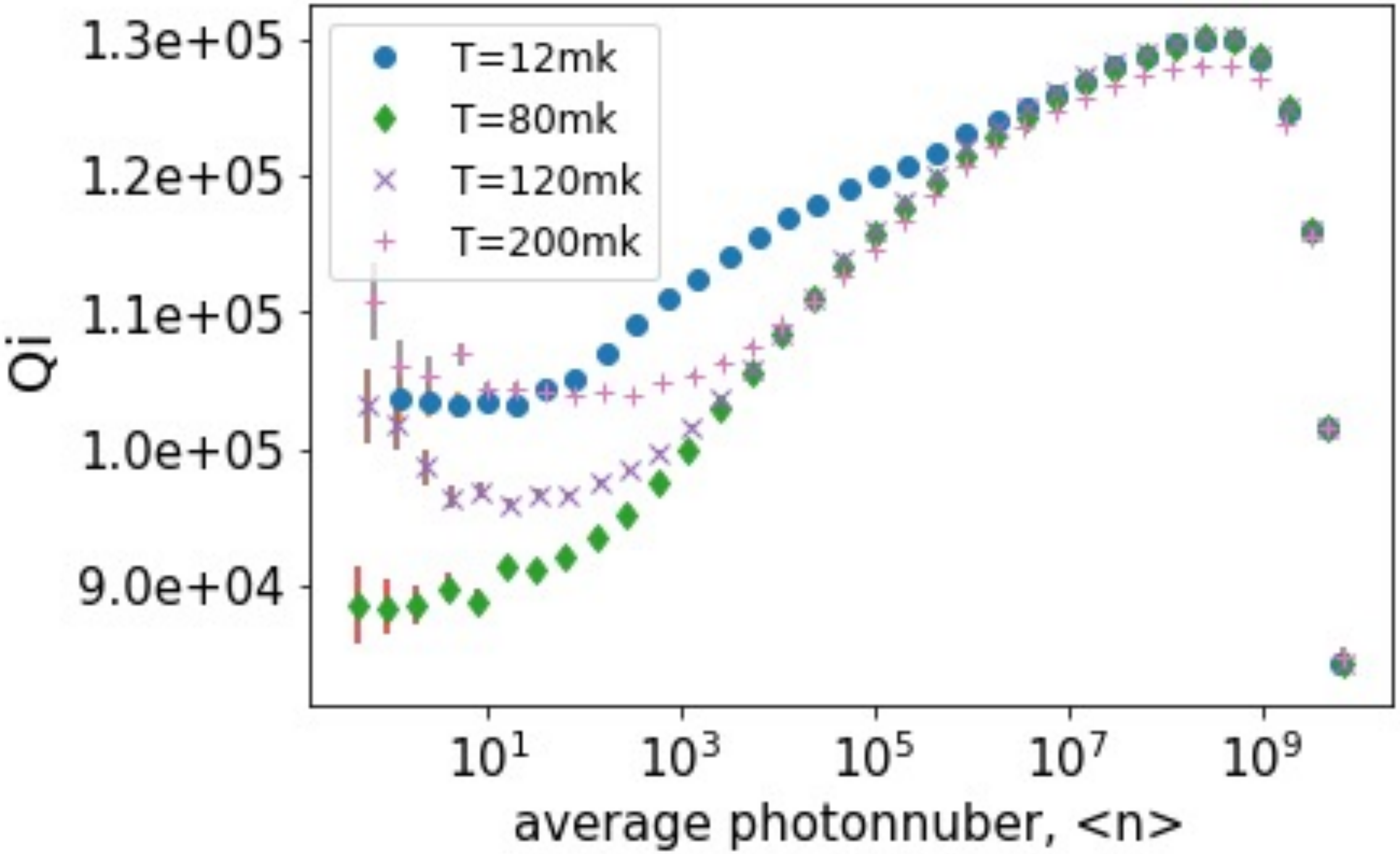

$$< n > \equiv \frac{4Q_L^2 P_{in}}{Q_c \hbar \omega_0^2}$$

Two Level System Losses

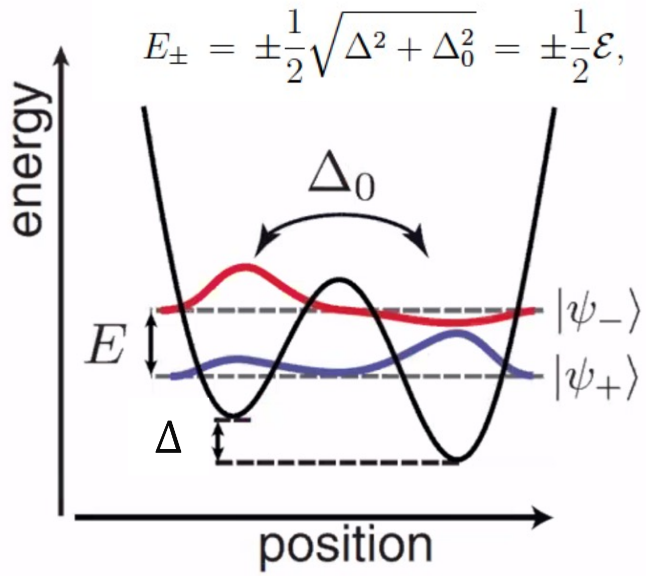

Schematic of a Two Level System[2]

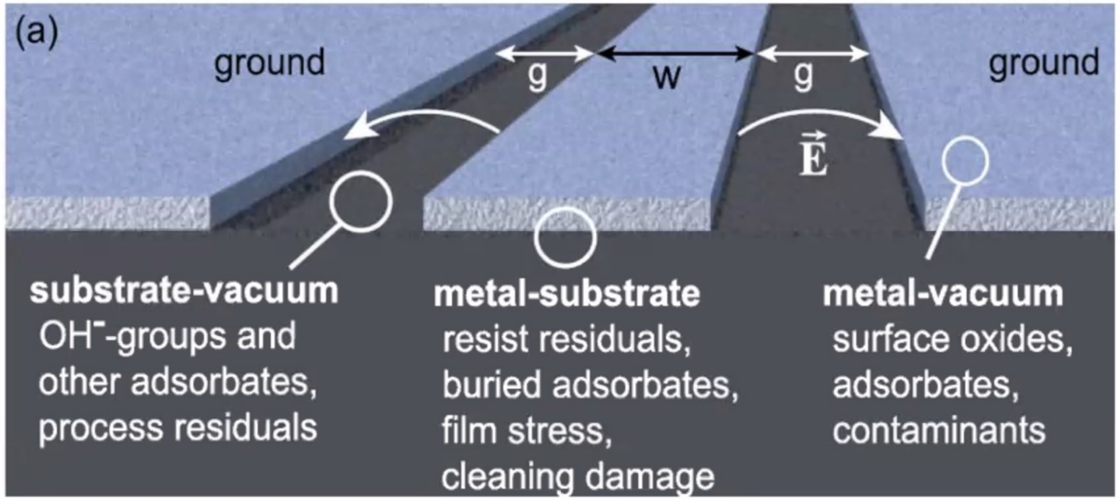

Muller Rep. Prog. Phys. (2019)

$$H_{TLS}=\begin{pmatrix} -\Delta & \Delta_0 \\ \Delta_0 & \Delta \end{pmatrix}$$

- **Sources of TLS**

1. Defects present in dielectrics at the metal/substrate/vacuum interface
2. Primarily associated with oxide layer/OH- groups/chemical residues

Contribution of TLS and Thermal Quasi Particles

$$\frac{f-f_n}{f_n} = F * \frac{\tan\delta}{\pi}\left\{Re\left[\Psi\left(0.5 - \frac{hf}{2\pi j k_b T}\right)\right] - \ln\left(\frac{hf}{k_b T}\right)\right\} - \frac{\alpha}{2}\sqrt{\frac{\pi\Delta_{s0}}{2k_bT}}\exp\left(-\frac{\Delta_{s0}}{k_bT}\right)$$

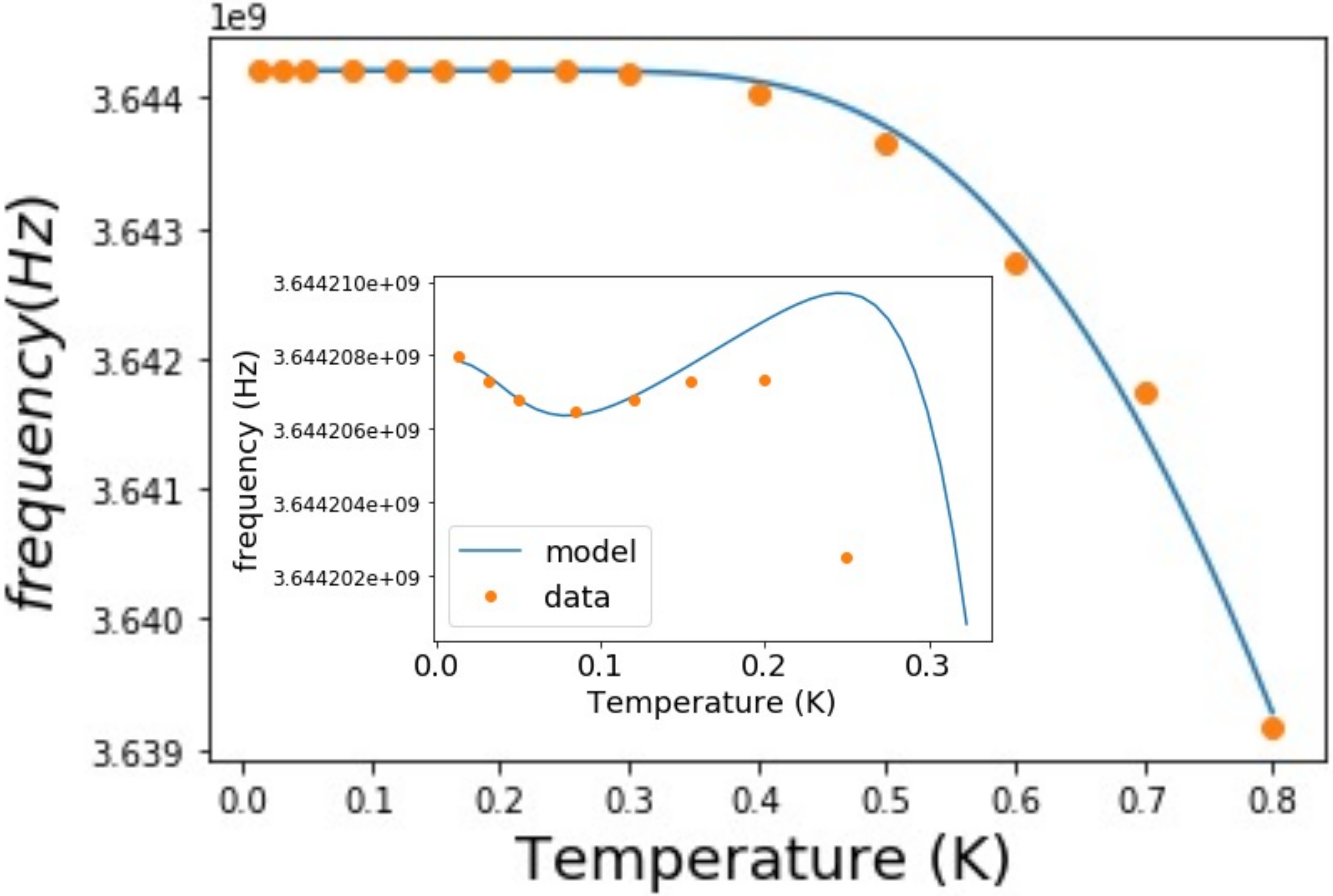

$$\alpha = \frac{L_k}{L_k + L_{geo}}$$

Fitting	Value
Δ_{S0} (μeV)	174.03 μ eV
α	0.0185
F	0.32
tanδ	2e-5 (sapphire)
f_n (GHz)	3.644

Contribution of Nonequilibrium Quasiparticles and Others

Δ - superconducting energy gap

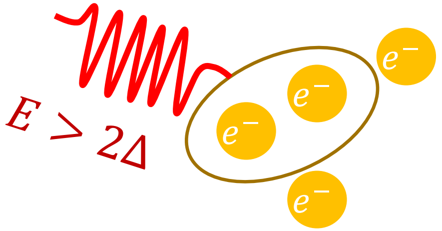

$E > 2\Delta$ breaks a Cooper pair forming 2 quasiparticles giving dissipation

Multi photon hν <2 Δ also generate quasiparticles

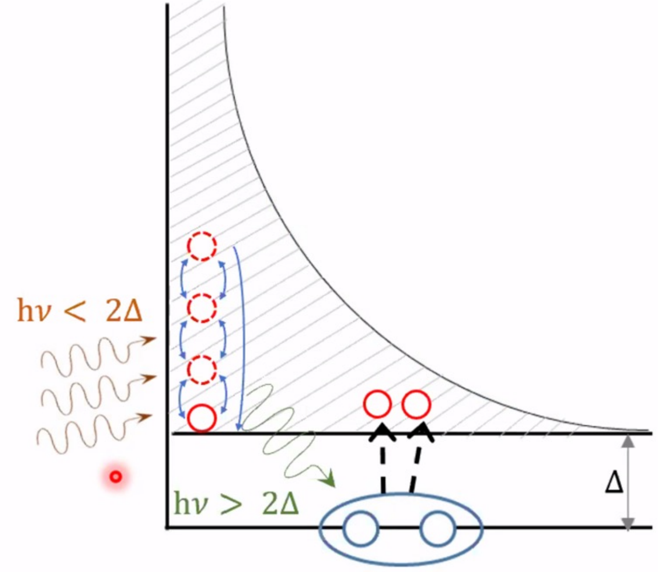

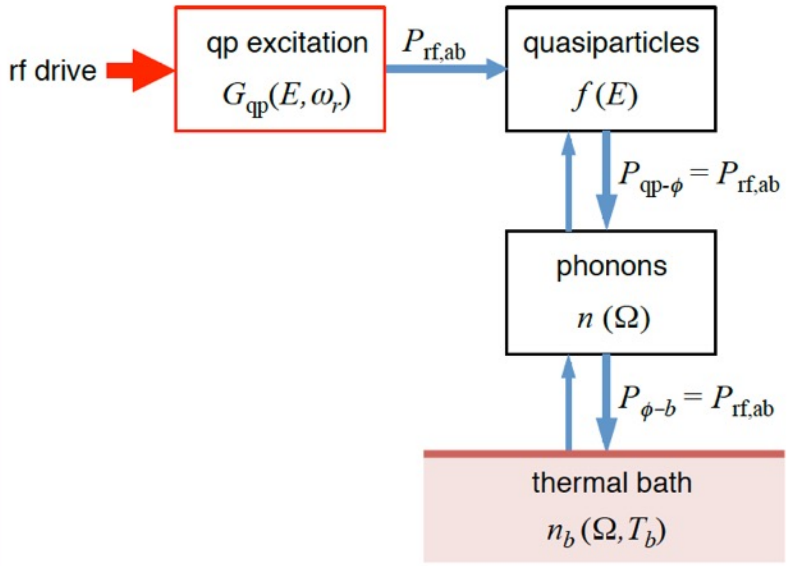

$$\frac{1}{Q_i} = \frac{1}{Q_{TLS}(T,E)} + \frac{1}{Q_{QP}(T,E)} + \frac{1}{Q_{vortices}(B)} + \frac{1}{Q_{rad}(w)}$$

Temperature Dependent Qi

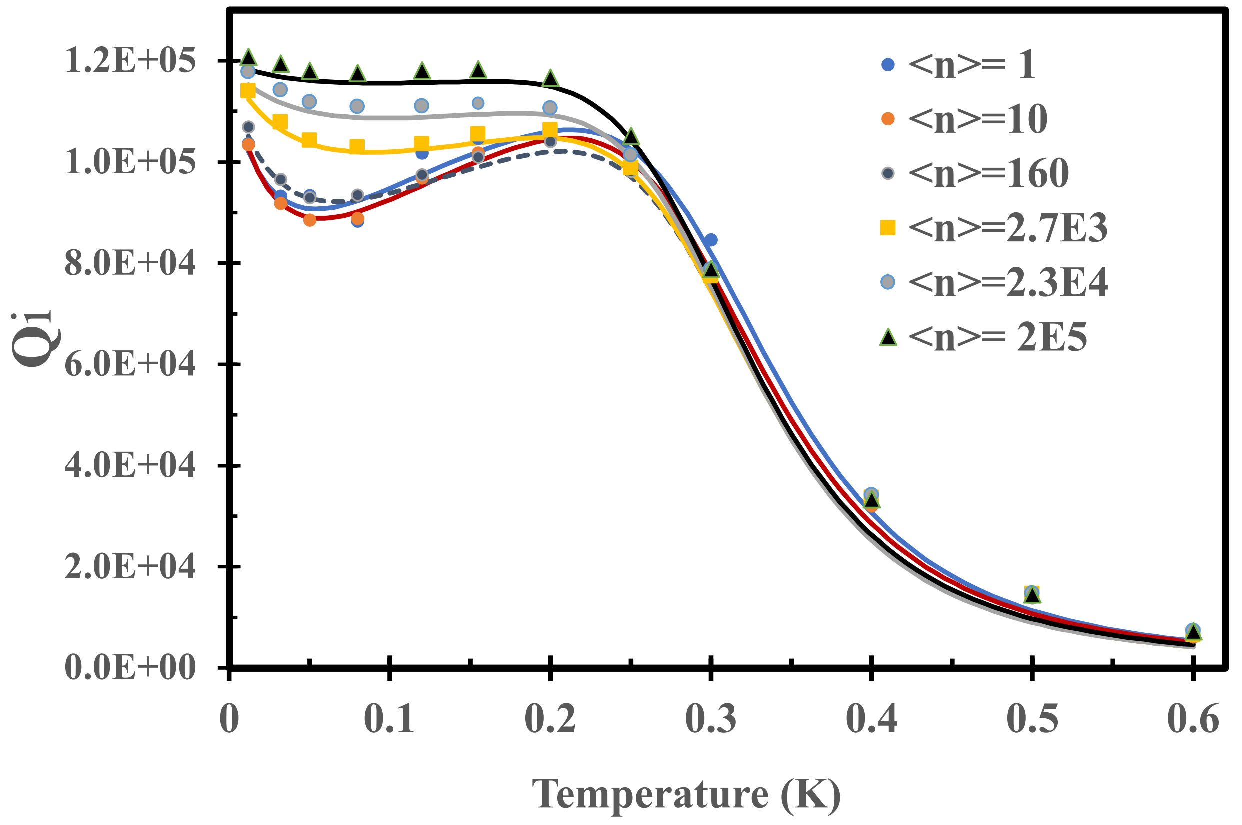

$$\delta_{TLS} = \frac{\delta^0_{TLS} \tanh\left(\frac{\varepsilon}{2k_BT}\right)}{\sqrt{1 + \frac{A}{T}\tanh\left(\frac{\varepsilon}{2k_BT}\right)}}$$

$$T_1 \sim \tanh\left(\frac{\varepsilon}{2k_BT}\right)$$

$$T_2 \sim 1/T$$

$$\frac{1}{Q_i} = \frac{1}{Q_{TLS}(T,E)} + \frac{1}{Q_{QP}(T,E)} + \frac{1}{Q_{other}}$$

Field Dependence of Fitting Parameter

$$\delta_{TLS} = \frac{\delta^0_{TLS}\tanh\left(\frac{\varepsilon}{2k_BT}\right)}{\sqrt{1+\frac{A}{T}\tanh\left(\frac{\varepsilon}{2k_BT}\right)}}$$

$$A = \frac{2d_0^2}{3}\left(\frac{1}{\Delta_0^2}\right)\left[\frac{r_L^2}{V_L^5}+\frac{r_T^2}{V_T^5}\right]^{-1} * \frac{2\pi\hbar^2}{\varepsilon} * \frac{\pi\hbar\rho^2V^2}{C\gamma Pk\Delta}$$ **E²**

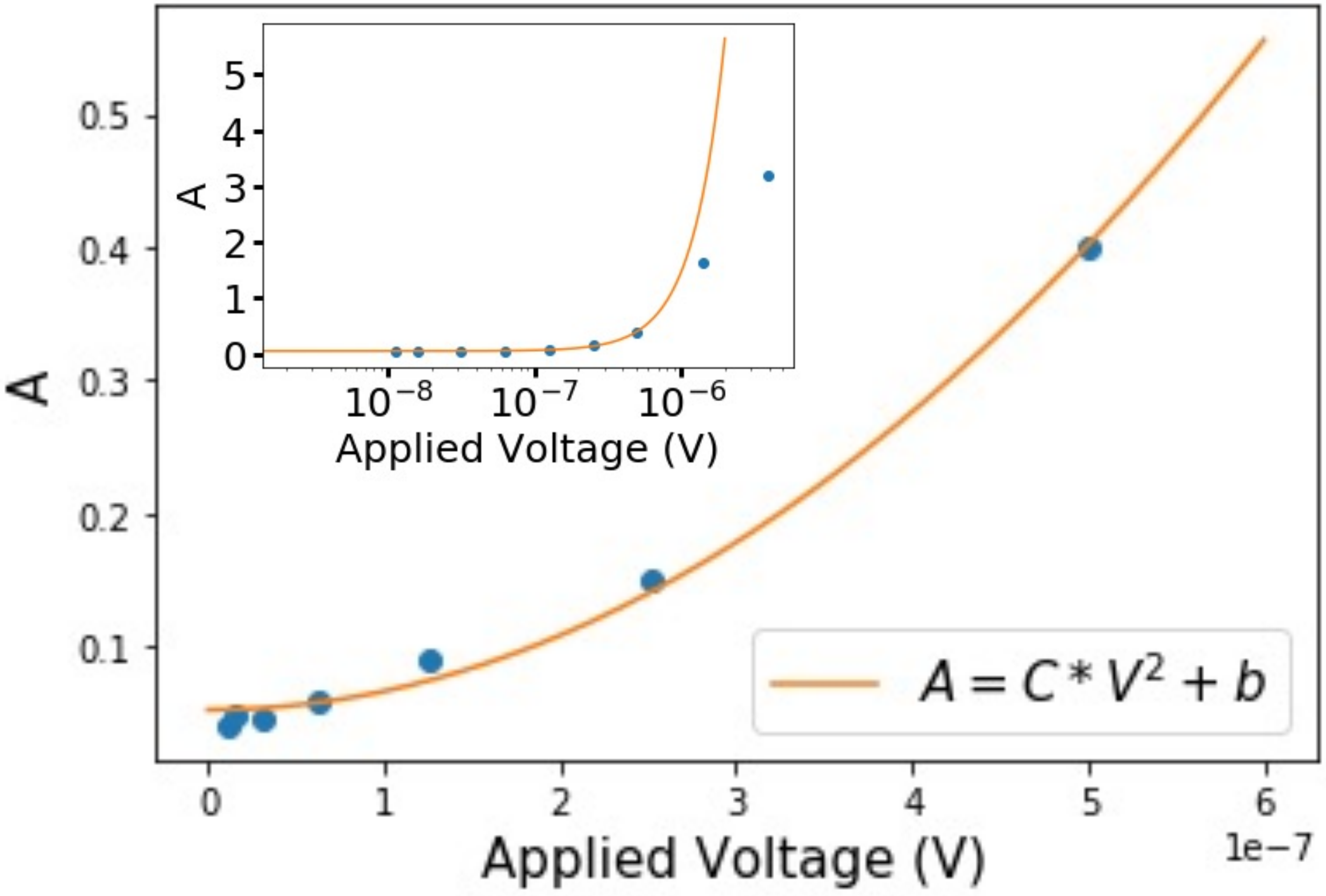

Dispersive Jaynes-Cummings Hamiltonian

$$\mathcal{H}_{\mathrm{JC}}^{(\mathrm{disp})} = \hbar(\tilde{\omega}_r + \chi\sigma_z)a^\dagger a + \frac{1}{2}\hbar\tilde{\omega}_q\sigma_z$$

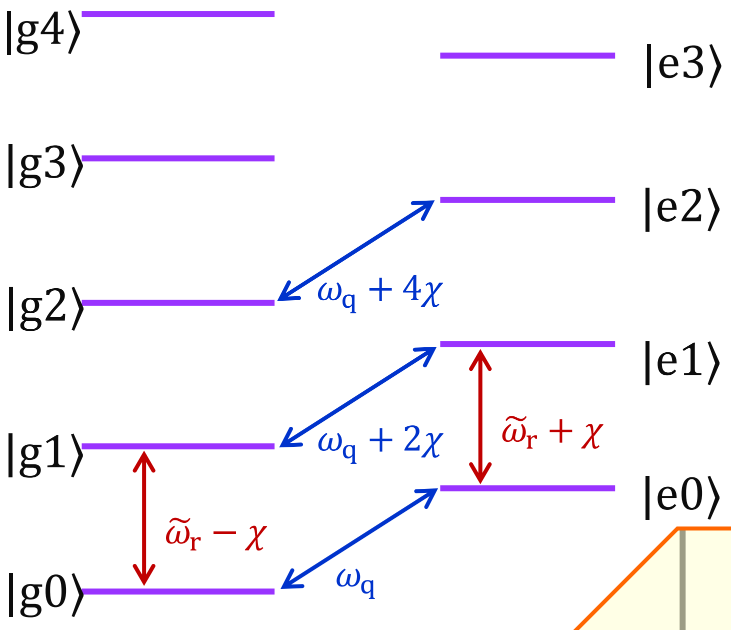

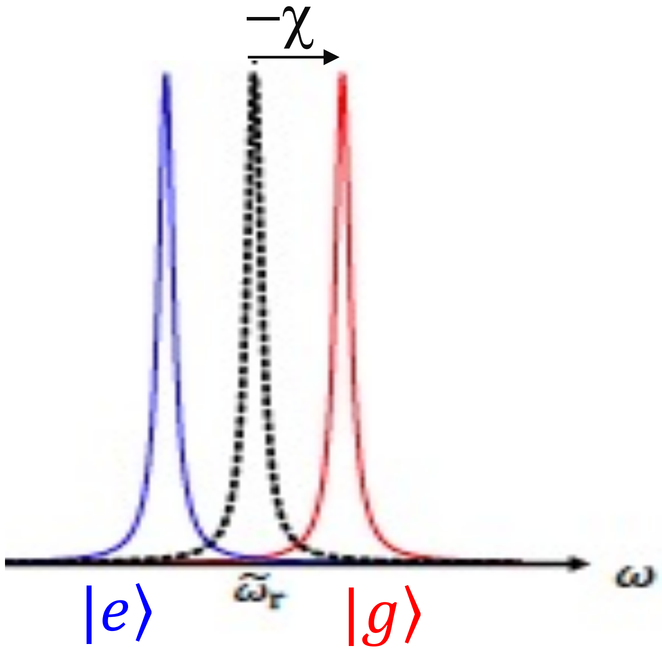

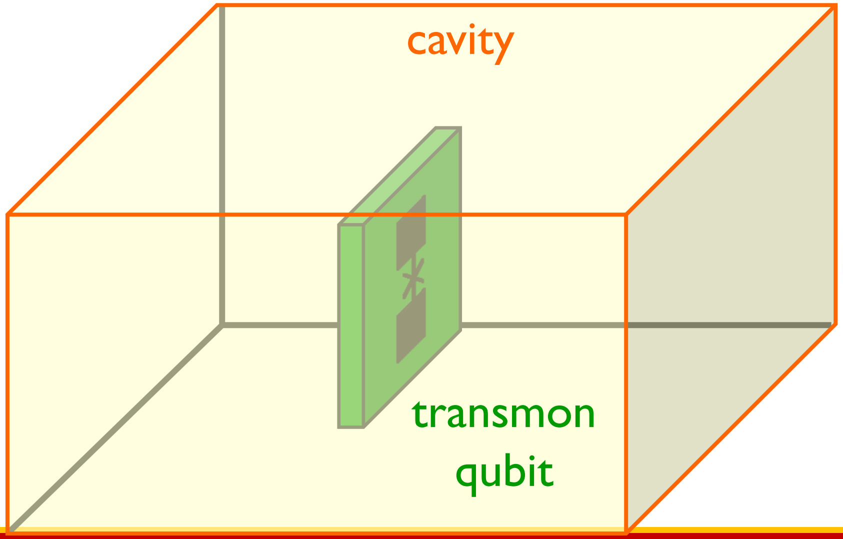

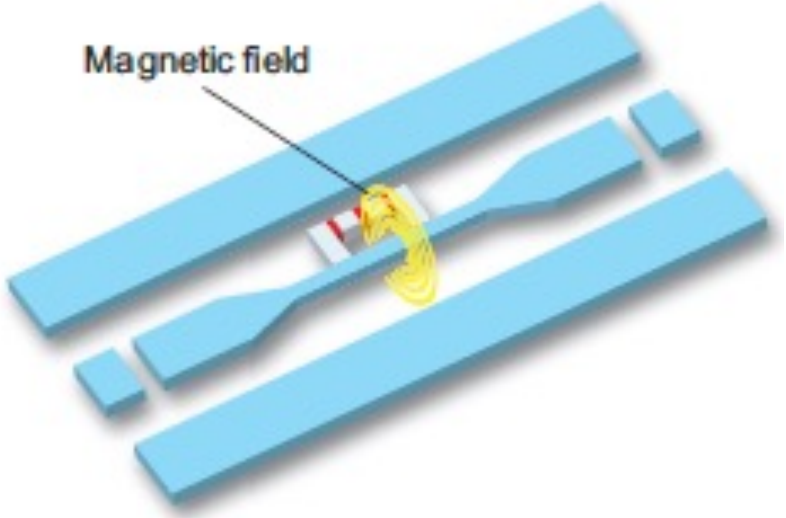

Driving the Qubit & Rabi Oscillations

Driving a qubit on resonance at frequency ω_{ge}

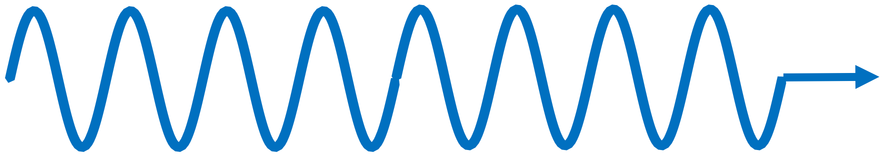

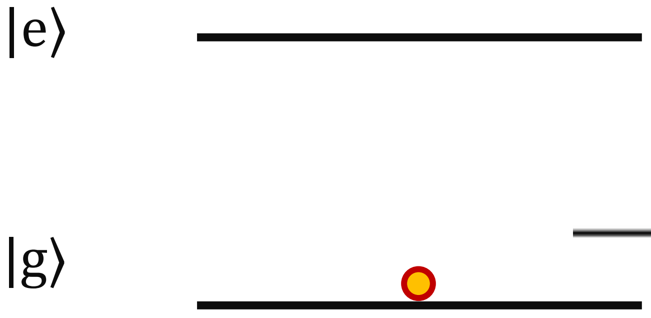

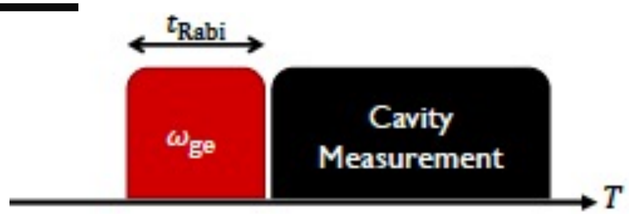

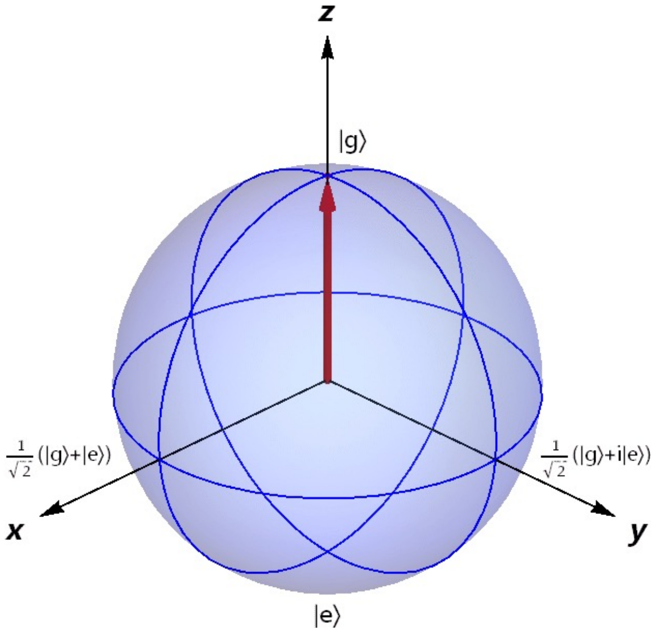

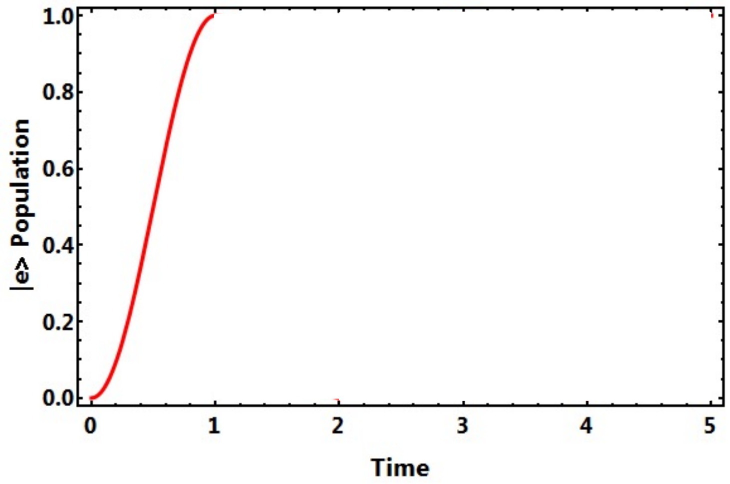

Driving a qubit on resonance at frequency ω_{ge}

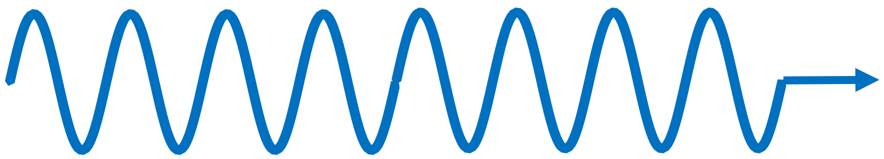

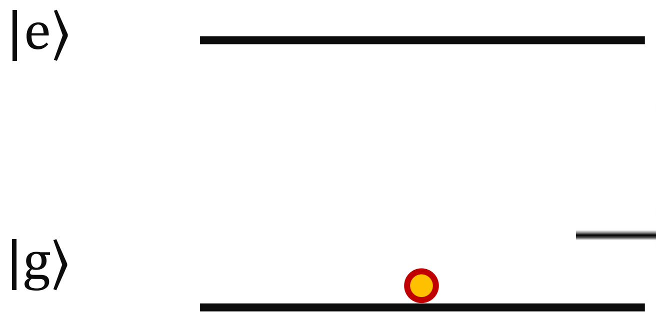

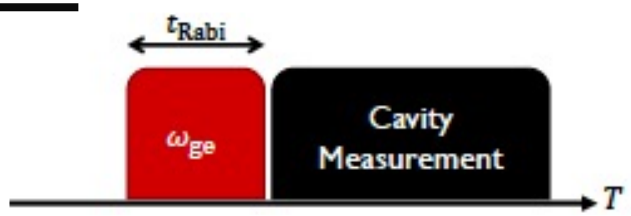

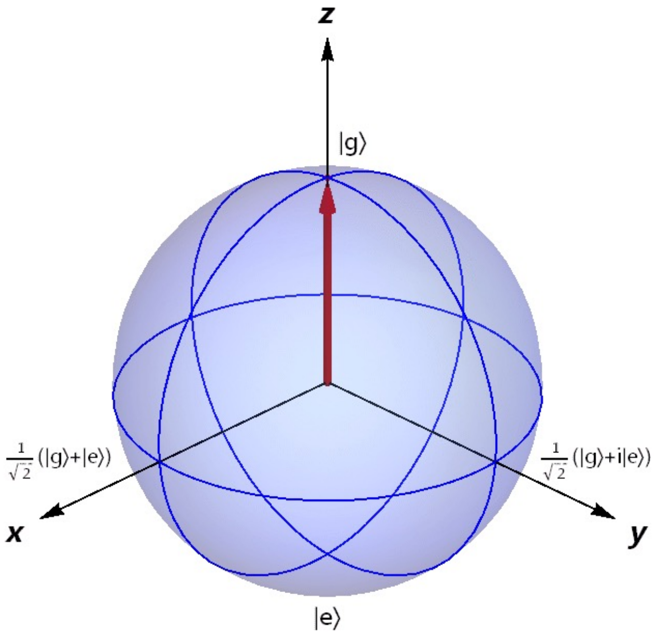

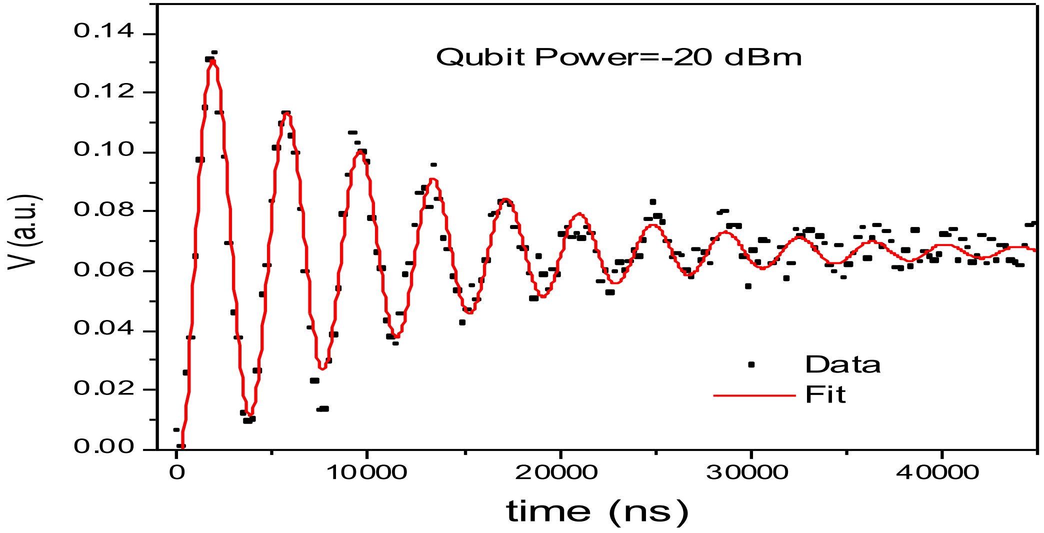

Transmon in 3D Cylindrical Cavities

Qubit Relaxation Measurement

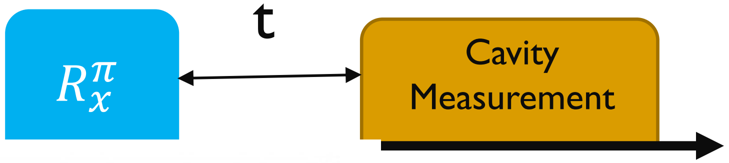

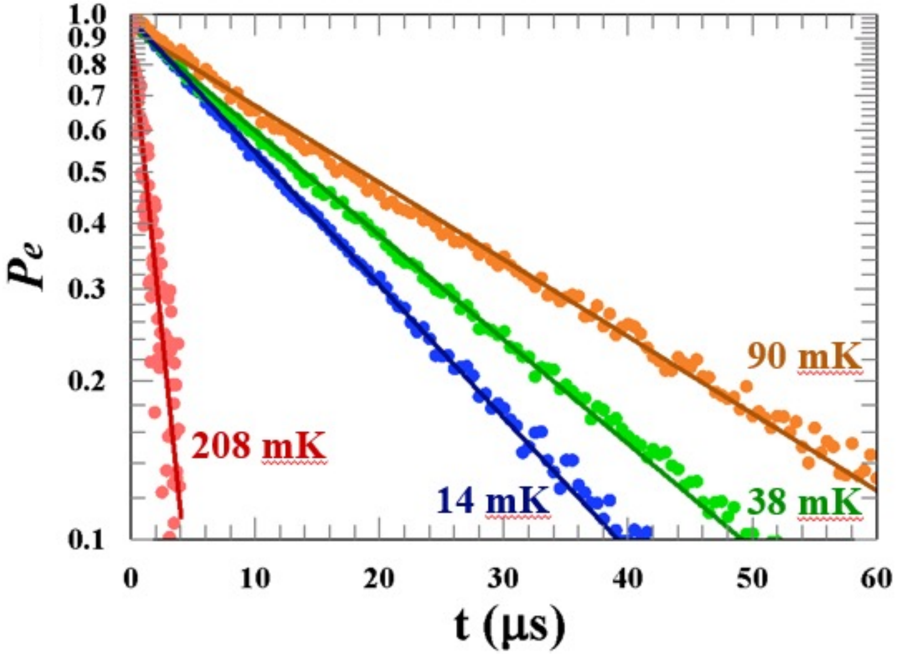

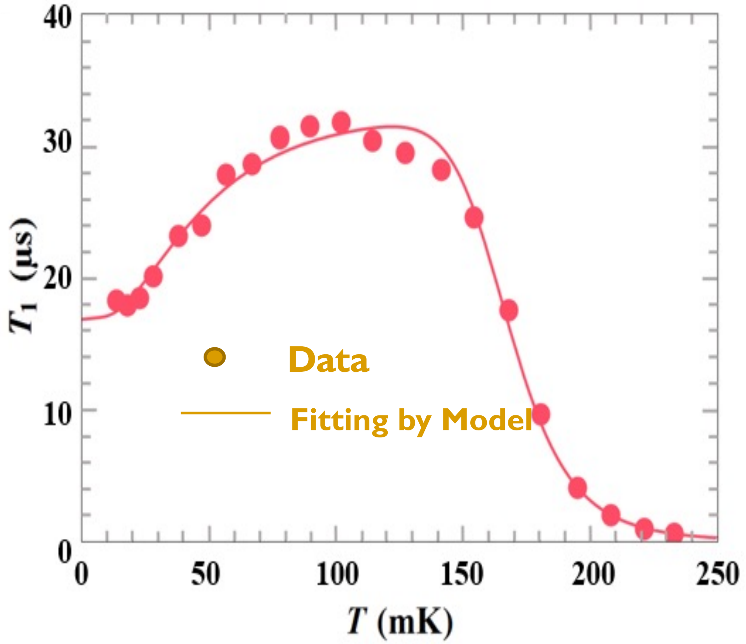

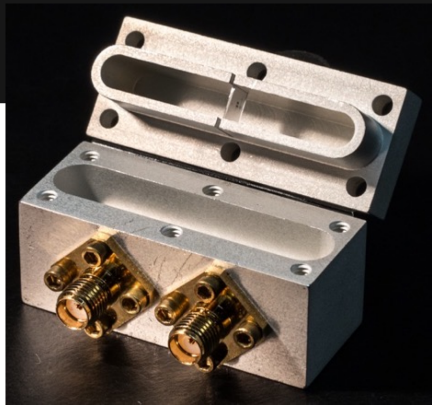

1. TLS Loss?

$$n_{2R} \approx n_{th,2} + \frac{n_{ne,1R}}{\sqrt{\frac{\Delta_1}{\Delta_2}}\exp\left(\frac{\Delta_2 - \Delta_1}{K_B T}\right) + \frac{\Omega_{2R}}{\Omega_{1R}}}$$

2. Imbalanced Nonequilibrium Quasiparticles at two different SC gaps?

$$n_{1L} \approx n_{th,1} + \frac{n_{ne,1L}}{1 + \frac{\Omega_{2L}}{\Omega_{1L}}\sqrt{\frac{\Delta_2}{\Delta_1}}\exp\left(\frac{\Delta_1 - \Delta_2}{K_B T}\right)}$$

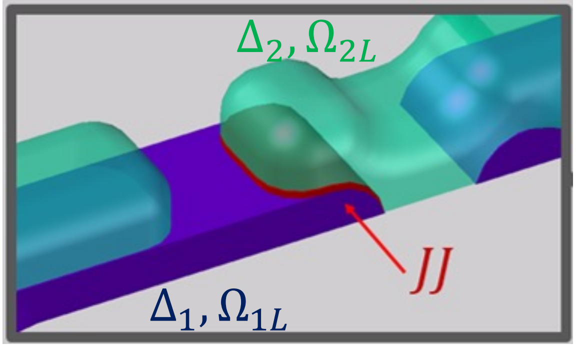

Motivation of Microwave Microscope

$$\frac{1}{Q_i} = \frac{1}{Q_{TLS}(T,E)} + \frac{1}{Q_{QP}(T,E)} + \frac{1}{Q_{rad}(W,geometry)} + \frac{1}{Q_{vortices}(B)} + \ldots$$

Develop a microscopy which can microscopically locate the place of loss at devices/cavities operating condition and identify the loss mechanism.

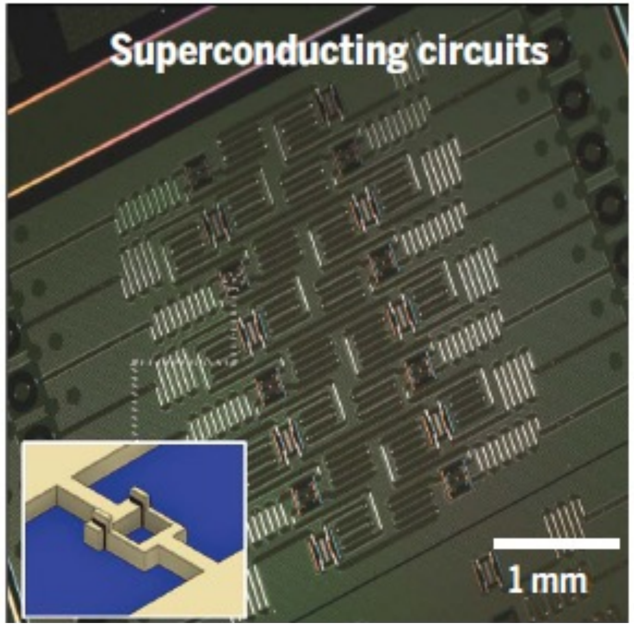

de Leon *et al.*, *Science* **372**, eabb2823 (2021) 16 April 2021

Laser Scanning Microwave Microscopy

1. Reflectance mode to generate a conventional image

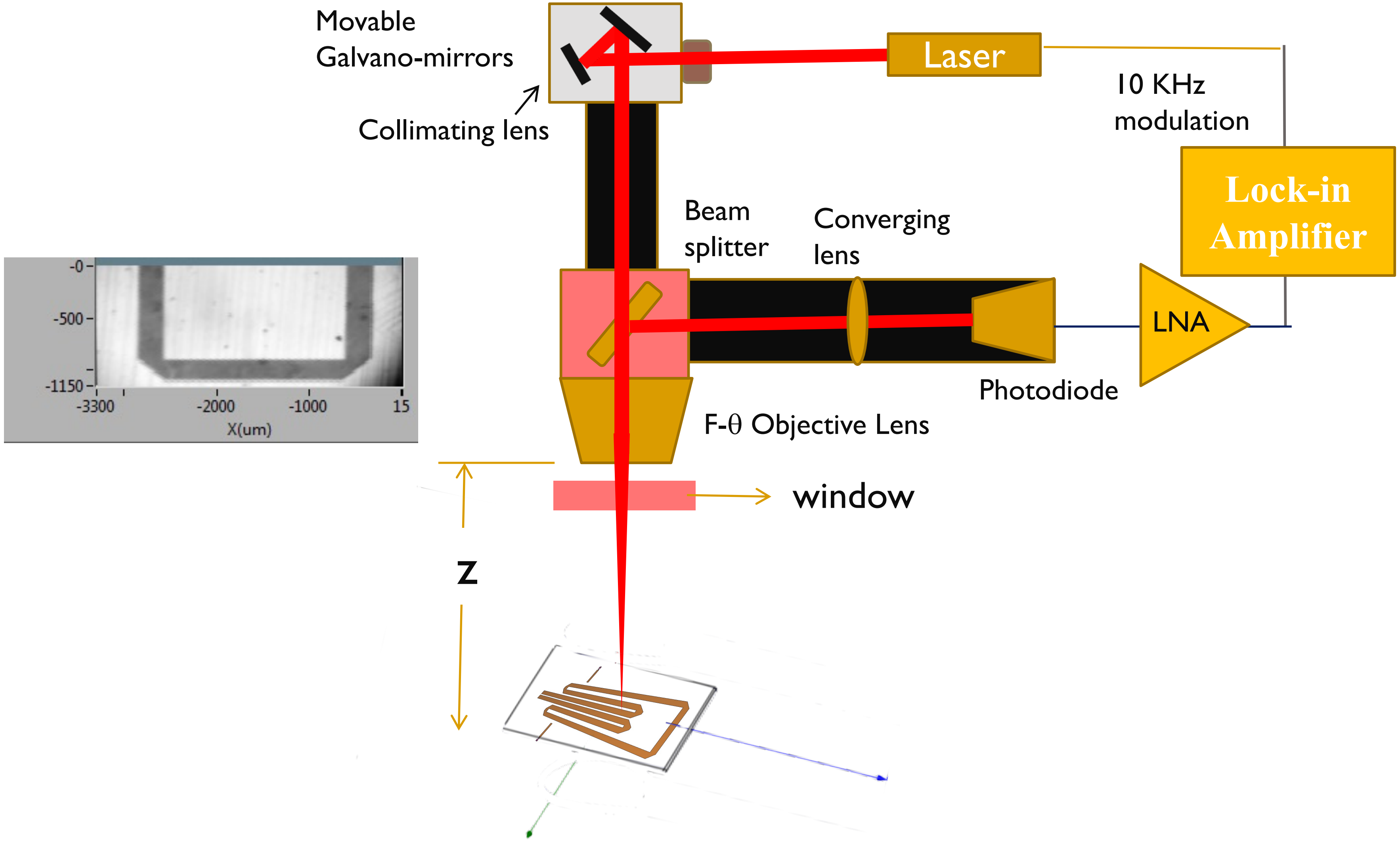

Laser Scanning Microwave Microscopy

2. Photoresponse mode to image the current density

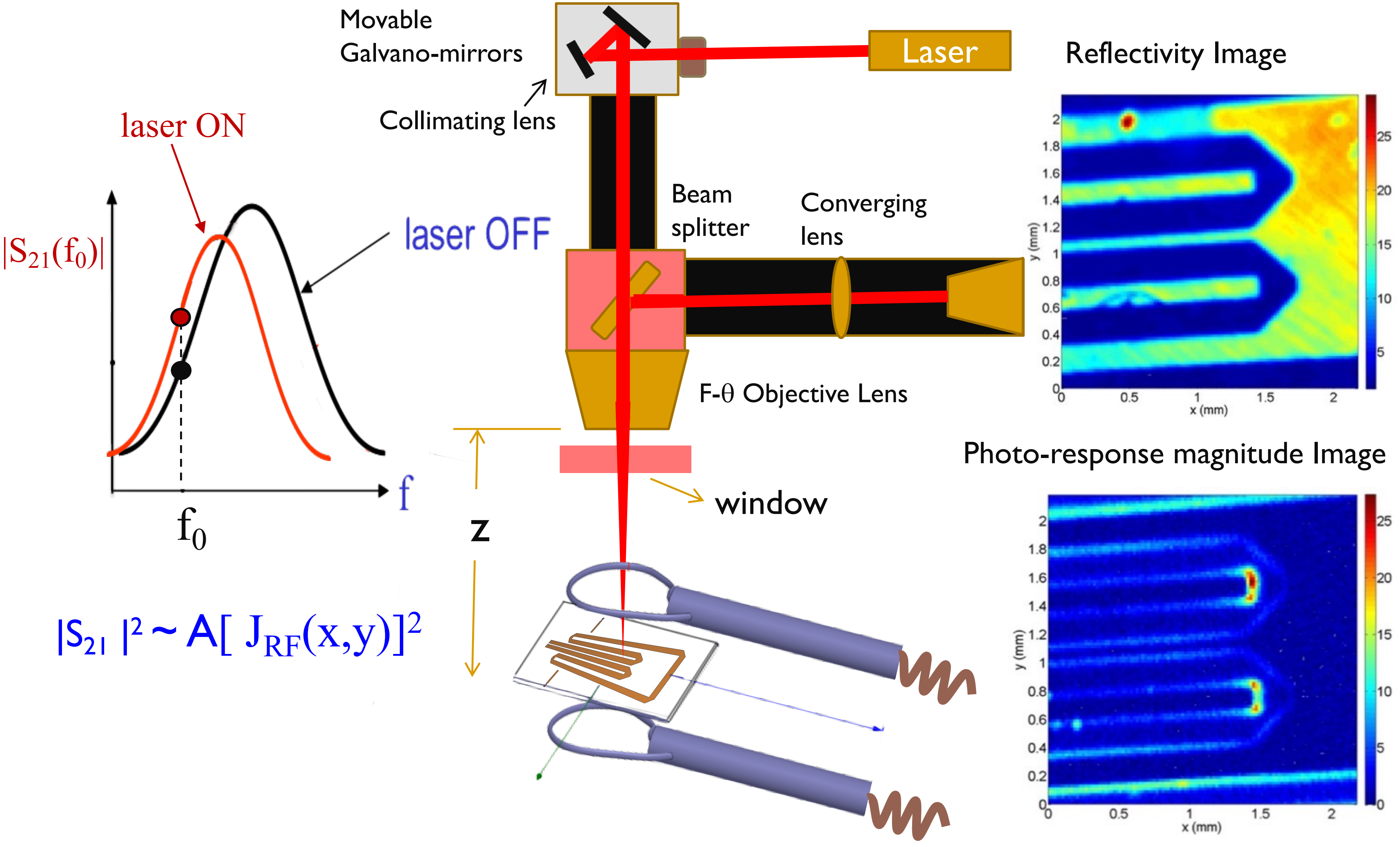

Near-Field Microwave Microscopy

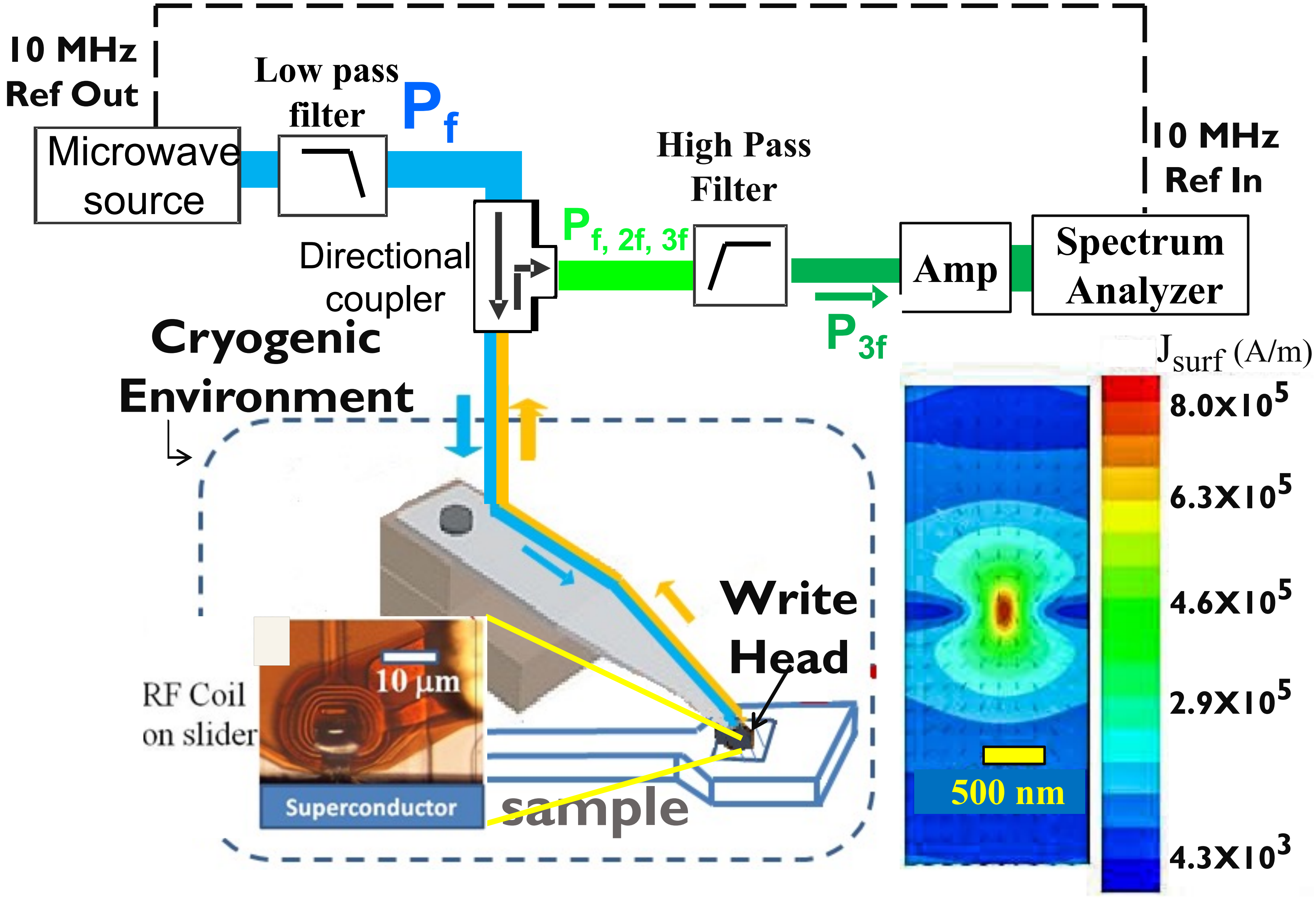

Nonlinear Measurement and Modeling

General curve of P_{3f} (P_f)

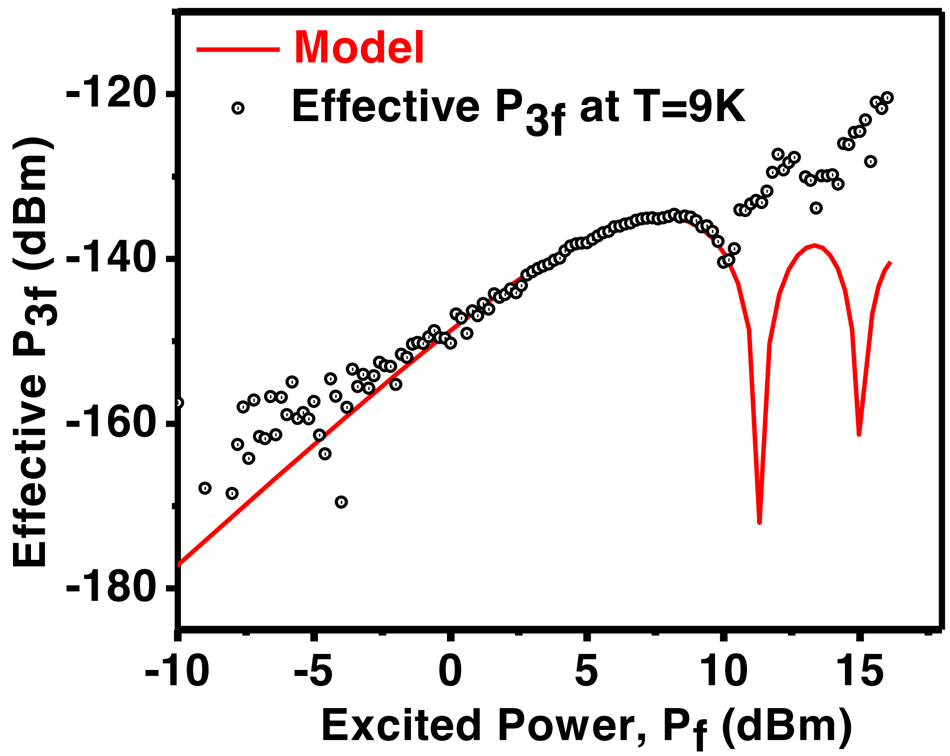

Tamin Tai et al , PRB **92, 134513 (2015)**

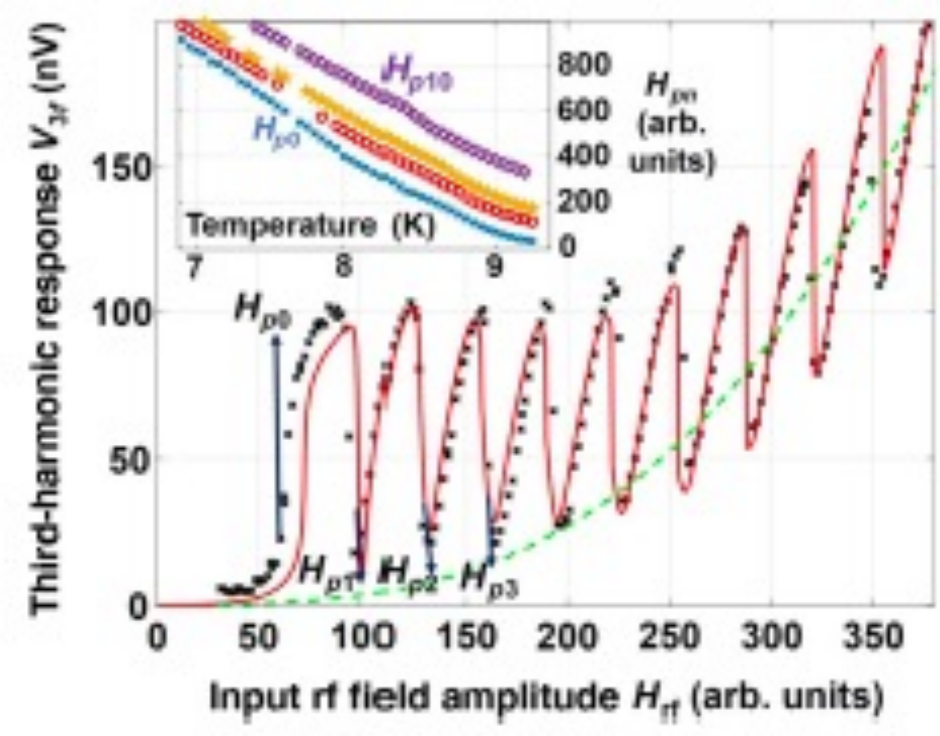

Bakhron Oripov et al.

PHYSICAL REVIEW APPLIED **11,** 064030 (2019)

Conclusions

❑ Superconducting Quantum Computing

❖ In aluminum resonator, an unusual increase of Qi with deceasing temperature is observed, which is due to the increase of TLS coherence time (T2) in ultra-low temperature and power.

❖ Temperature dependent of T1 on transmon qubits is also affected by many loss issues. In addition to TLS loss issue, two gaps model also can interpret the T1 temperature dependent behavior.

❑ Microscopy

❖ **Laser Scanning Microscopy**

A clear photo response with the capability of phase-sensitive measurement of local microwave properties on YBCO resonators are obtained by LSM with ~ μm length resolution.

❖ **Near-field Scanning Microwave Microscopy**

This microscopy achieved local harmonic generation from bulk Nb surfaces from sub-micron scale length and the measured nonlinearity is interpreted by the model of weak-link Josephson junctions.